Journal of Theoretical Biology 315 (2012) 53–63

Contents lists available at SciVerse ScienceDirect

Journal of Theoretical Biology

journal homepage: www.elsevier.com/locate/yjtbi

In silico docking reveals possible Riluzole binding sites on Nav1.6 sodium channel: Implications for amyotrophic lateral sclerosis therapy

Omar Sierra Bello [a], Janneth Gonzalez [a], Francisco Capani [b], George E. Barreto [a,*]

[a] Departamento de Nutrición y Bioquímica, Facultad de Ciencias, Pontificia Universidad Javeriana, Bogotá, DC, Colombia
[b] Laboratorio de Citoarquitectura y Plasticidad Neuronal, Instituto de Investigaciones Cardiológicas, Buenos Aires, Argentina

HIGHLIGHTS

- Riluzole acts on Nav1.6 sodium channel.
- Riluzole interacts with the Nav1.6 channel on TYR 1787, LEU 1843 and GLN 1799 residues.
- The prediction may be used an output for better drug design therapy in ALS.

ARTICLE INFO

Article history:
Received 10 April 2012
Received in revised form
31 August 2012
Accepted 6 September 2012
Available online 18 September 2012

Keywords:
ALS
Nav1.6
Riluzole
GLN 1799

ABSTRACT

Amyotrophic lateral sclerosis (ALS) is a common neurodegenerative disorder characterized mainly by a progressive loss of motor neurons. Glutamate excitotoxicity is likely the main cause of neuronal death, and Riluzole interferes with glutamate-mediated transmission. Thus, in such independent pathway, these effects may be partly due to inactivation of voltage-dependent sodium channels. Here we predict the structural model of the interaction and report the possible binding sites of Riluzole on Nav1.6 channel. The docked complexes were subjected to minimization and we further investigated the key interacting residues, binding free energies, pairing bridge determination, folding pattern, hydrogen bounding formation, hydrophobic contacts and flexibilities. Our results demonstrate that Riluzole interacts with the Nav1.6 channel, more specifically in the key residues TYR 1787, LEU 1843 and GLN 1799, suggesting possible cellular implications driven by these amino acids on Riluzole–Nav1.6 interaction, which may serve as an important output for a more specific and experimental drug design therapy against ALS.

1. Introduction

Amyotrophic lateral sclerosis is a common adult neurodegenerative disorder (Hoffman, 2008). It is mostly characterized by a progressive loss of motor neurons in the cerebral cortex and spinal cord causing weakness, atrophy, paralysis, and death from respiratory failure within a few years on average (Andrews, 2009). Since its discovery in 1874 (Norris et al., 1989), ALS has remained a mystery, and probable causes, cure or effective treatments for this diseases are still unknown (Clark et al., 2005).

Oxidative stress, formation of soluble aggregates by immature superoxide dismutase, growth factor deficiency and disruption of neurofilaments are thought to be the main causes of ALS (Cheah et al., 2010). However, a previous study also pointed glutamate excitotoxicity to be the likely the cause of death of motor neurons (Van Den Bosch et al., 2006). A previous report showed that the Na^+ channel blockade may increase motor neurons survival against excitotoxic death by targeting the sodium channel protein Nav1.6 (Hebert et al., 1994), suggesting a possible implication of these channels in the neuropathology of ALS.

Voltage-gated sodium channels (VGSc) are assemblies of one alpha helix and one or more beta, becoming heterometric subunits (Tarnawa et al., 2007). Alpha subunits are heavy proteins (about 260 kDa) containing four homologous domains which contribute to the formation of the inner lining of the channel (Diss et al., 2001). An activation of these channels carries a cell depolarization, which leads to sodium influx and a persistent depolarization dysregulates the osmotic balance of the cell, as intracellular sodium concentration rises (Wang et al., 2008). The entry of sodium ions, water and chloride ion in order to maintain ionic equilibrium induces osmotic swelling (Shashank, 2003) and the release of glutamate into the extracellular milieu, leading to pronounced neuronal death by excitotoxicity (Foran and Trotti, 2009).

Nowadays, Riluzole "trademark Rilutek®"(Knox et al., 2010), the most used drug for treating ALS, is a benzothiazole derivative (Ahn et al., 2005) that interferes with glutamate-mediated transmission in the central nervous system (Tavakoli, 2002). It is the only drug approved by the FDA (Food and Drug Administration), which

* Corresponding author. Tel.: +57 1 320 8320x4096/4137.
E-mail address: gsampaio@javeriana.edu.co (G.E. Barreto).

0022-5193/$ - see front matter © 2012 Elsevier Ltd. All rights reserved.
http://dx.doi.org/10.1016/j.jtbi.2012.09.004

improves survival rates of patients with ALS (Araki et al., 2001). As a known inhibitor of glutamatergic neurotransmission, Riluzole is a potent neuroprotective agent with anticonvulsant, anxiolytic, anesthetic, sedative and anti-ischemic properties (Aggarwal and Cudkowicz, 2008). For instance, the drug acts on excitatory amino acid neurotransmission through at least four mechanisms, being the most important an inhibition of the release of glutamate due to the inactivation of voltage-dependent Na^+ channels on glutamatergic nerve terminals (Ajroud-Driss et al., 2007). Riluzole reversibly blocks Na^+ channels, with its specific target being the voltage-gated sodium channel alpha subunit, Nav1.6 (Knox et al., 2010). Furthermore, Riluzole may also antagonize persistent Na^+ currents by 46% (Donovan et al., 2011) and afford neuroprotection by reducing intrinsic motor neuronal excitability (Cheah et al., 2010), in addition to dampening the susceptibility of motor neurons to potential Na^+-induced insults (Tarnawa et al., 2007). A previous study showed that anti-glutamatergic properties of Riluzole were merely downstream manifestations of its Na^+ channel-blocking properties (Yiangou et al., 2007), suggesting an indirect effect of this drug on glutamate transporters (Cheah et al., 2010).

Many concerns are still unresolved due to experimental caveats (Dunlop et al., 2003), the lack of significant theoretical guidance (Fu et al., 2002) and experimental data on the structure of Riluzole–VGSc complexes (Tarnawa et al., 2007). Thus, the majority of marketed drugs that act on ion channels were discovered empirically rather than by molecular insights, and most of them have shown serious side problems and doubtful efficacy (Fu et al., 2002). For instance, it has been shown that inhibition of the voltage-gated sodium channel is crucial for excitotoxicity withdrawn in ALS patients (Van Den Bosch et al., 2006; Karp, 2001; Bahram et al., 2001), and that possible Riluzole binding site is thought to be on the alpha subunit of the sodium channel (Song et al., 1997). These reports suggest that stabilization of the inactivated state of this channel may underlie the neuroprotective properties of Riluzole. On the other hand, studies on the motor cortex of ALS patients have shown that accumulation of intracellular sodium, as a result of trauma-induced perturbation of voltage-sensitive sodium channel activity, is a key early mechanism in the secondary injury cascade (Schwartz and Fehlings, 2002). Although some experimental studies have shed light on the ALS pathological and molecular driven mechanisms, computational simulations at the molecular level may be considered as a potent tool to better understand electrophysiological parameters (Wokke, 1996) performed on voltage-gated sodium channel aiming at discovering possible binding sites of neuroprotective molecules for designing better and specific drugs for treating neurodegenerative diseases (Dunlop et al., 2003), such as ALS (Azbill et al., 2000).

In this study, we have integrated a docking analysis and homology modeling to understand the association of the Riluzole with the alpha subunit of voltage-gated sodium channel Nav1.6 (McGuire et al., 1997). First, we have constructed the three-dimensional (3D) structure model for the voltage-gated sodium channel alpha subunit Nav1.6 by homology modeling, taking the X-ray crystal structure of the sodium channel protein type 2 alpha subunit (PDB: 2KAV) as a template. The docking analysis and homology modeling were employed to localize binding sites to identify residues involved in the complex formation and to estimate the binding affinity and infer possible biological meaning of the sodium channel Nav1.6 with Riluzole.

2. Materials and methods

2.1. Atomic coordinates and amino acids sequence

The amino acid sequence of the voltage-gated sodium channel subunit alpha Nav1.6 was obtained from the Swiss-Prot database (http://expasy.org/sprot%20database; entry number: O88420.1; (Bairoch and Apweiler, 1997). The atomic coordinates of the human voltage-gated sodium channel, brain isoform (Nav1.2) was obtained from the Brookhaven Protein Database PDB entry: 2KAV (Berman et al., 2000).

2.2. Molecular modeling

Since the crystal structure of the sodium channel protein type 3 alpha subunit Nav1.6 was not previously determined (Wang et al., 2008), BLAST (basic local alignment search tool (Altschul et al., 1997), sequence analysis was performed against the whole protein data bank to detect homologous/analogous protein templates by matching the whole-chain sequences of target subunits to solved protein structures. Multiple sequence alignment was performed by ClusterW2 (Thompson et al., 1994). From the results obtained from BLAST (Altschul et al., 1997), human voltage-gated sodium channel Nav1.2 was selected as template. The 3D structure model of the alpha channel subunit was generated by the biopolymer homology modeling software—Esypred3D (Lambert et al., 2002). Following this approach, the generated model was validated using the PROCHECK program (Laskowski et al., 1993) and compared with the previous secondary structure predictions for the helix of each subunit at the level of the length of the secondary structure. The aim of PROCHECK (Laskowski et al., 1993) is to assess how normal or, conversely, how unusual the geometry of the residues in a given protein structure is compared to the stereochemical parameters of well-refined and high-resolution structures (Morris et al., 1992).

2.3. Prediction of binding sites

The possible binding sites of selected target receptor was assessed using Q-site finder (Laurie and Jackson, 2005) to predict ligands binding site and also whole protein structure assumed as a binding site. Q-site finder works by binding hydrophobic probes to the protein and finding clusters of probes with the most favorable binding energy (Laurie and Jackson, 2005). These include active sites located on protein surfaces and voids buried in the interior of proteins. Q-site finder includes a graphical user interface, flexible interactive visualization, as well as on-the fly calculation for user-uploaded structures. The physical and chemical properties of the Riluzole were retrieved from Drug Bank database (Knox et al., 2010).

2.4. Folding pattern determination of the VGSc Nav1.6

Protein folding is the process by which a protein structure assumes its functional shape or conformation (Balamurugan et al., 2011). The correct three-dimensional structure is essential to determinate its function, and becomes very important to understand its properties, functions and biologic state. We used PFP-Pred to locate the folding patterns of the selected protein (VGSc Nav1.6 homology model) by hydrophobic analyses of the protein and looking for clusters of probes with the highest favorable binding energy (Balamurugan et al., 2011).

2.5. Computation of flexibilities of VGSc Nav1.6 homology model and Riluzole

Normal mode analysis (NMA) is a powerful tool for predicting possible flexibilities of a given macromolecule. We used El Némo (elastic network model; (Suhre and Sanejouad, 2004)), a web interface to measure the flexibilities of the Riluzole upon binding to the channel during docking simulations.

2.6. Molecular docking simulations

The docking analyses of Riluzole were carried out with Autodock v4.2 program (Autodock, Autogrid, Autotors, Copyright-1991e2000), from the Scripps Research Institute (http://www.scripps.edu/mb/olson/doc/autodock). To run Autodock we used a searching grid extended over the selected target protein to delimitate the docking area. The polar hydrogens were added to the ligand moieties, as well as Kollman charges were assigned and atomic solvation parameters were added. Polar hydrogen charges of the Gasteiger-type were assigned and the nonpolar hydrogens were merged with the carbons and the internal degrees of freedom and torsions were set. Riluzole was docked to all of the target protein complexes with the molecule considered as a rigid body being flexible. Affinity maps for all the atom types, as well as an electrostatic map, were computed with a grid spacing of 0.375 E. The search was carried out with the Lamarckian genetic algorithm selected in Autodock.

2.7. Explicit solvent simulations

When predicting simulations of molecules in liquid environments, it becomes computationally convenient to approximate the electrostatic effects of the solvent by a continuum dielectric model (Cornell et al., 2001). In this approximation, only the intrasolute electrostatic interactions need to be evaluated (Cornell et al., 1995). This strongly increased the number of interactions with respect to a non-explicit treatment of the solvent and explains in a better way the direct and non-direct contacts in a liquid environment (Cornell et al., 2001).

For the explicit solvent simulations we used UCSF Chimera (Pettersen et al., 2004), an extensible program for interactive visualization and analysis of molecular structures and related data, including solvent analysis and conformational ensembles (Pettersen et al., 2004). We used a force field50 and the TIP3 model for water. Long-range electrostatic interactions were handled by the PME method, using the recommended Amber accuracy parameters (Cornell et al., 1995). This implies a limit for the real-space non-bounded interactions of 8 Å, and about a 1 Å grid spacing for the reciprocal space calculations. The added solvent molecules such that the minimum distance of a protein atom to the edge of the rectangular box was 10 Å (Tsui and Case, 2000). This procedure added 9.697 water molecules in the predicted model of the voltage gated sodium channel Nav1.6.

We also generated a graphic comparing and validating the fluctuation of both structures (homology modeled structure – implicit solvent structure) and direct – indirect contacts for the implicit solvent structure (Gerber et al., 2000) by means of the UCSF Chimera and a calculation of the RMSD value (Pettersen et al., 2004).

2.8. Refinement and complex validation

To avoid steric overlaps and clashes, the screened docking solutions were submitted to an energy minimization performed by using MacroModel software (MacroModel, 2011). We worked with the PRCG (Polak–Ribiere conjugate gradient) algorithms with a consistent valence force field (CVFF). We set a convergence criterion for minimization of a gradient to <0.05 kJ/Å-mol for quality test of protein–ligand (VGSc–Riluzole) complex and docking performance. The server Astex Diverse were used as a restriction and qualifier of the final docking solutions (Hartshorn et al., 2007).

2.9. Computation of the binding free energy

The binding free energy of the channel and the Riluzole were assessed by DFIRE software (Liu et al., 2004) for estimation of the binding affinity. The correct 3-D structure of a protein is often dependent on an intricate network of H bonds and hydrophobic contacts (Wallace et al., 1996). Polar contacts assessment was performed using the molecule Viewer PyMOL. The results are displayed on the docking solutions (Fig. 6) proving the affinity of the contacts, indicating how strong the contacts of the Riluzole with the voltage-gated sodium channel are and how they are interacting.

2.10. Transmembrane residues

The voltage-gated sodium channels alpha subunits are organized in four homologous domains, each one being composed of six transmembrane segments (S1–S6; (Tytgat and Peigneur, 2012)). The pore region is formed by the S5 and S6 segments as previously reported (Duclohier, 2009). Sequence alignment with the transmembrane amino acid sequence of the reported Nav1.2 crystal structure and the Nav1.6 homology model was performed to identify the transmembrane segment of the protein and to compare with the docking simulation and the Riluzole binding site.

3. Results

3.1. Structure of VGSC alpha subunit Nav1.6

First, a Blast request was performed against the whole PDB to select the template by which could be used to generate a model of the voltage-gated sodium channel Nav1.6 (Fig. 1). The voltage-gated sodium channel, brain isoform (Nav1.2 PDB: 2KAV) primary structure showed the best scores. Furthermore, the 3D-structure of the generated model was similar to that of the template with RMSD (Ramachandran) value of 0.628 Å for the best structure.

In the NCBI, the VGSC alpha subunit Nav1.6 is found as sodium channel protein type 5 alpha subunit, which is a protein of 2016 aa reported on October 19 2011 (accession number: Q14524; Query ID: (gi|328506973|gb|AEB21639.1|). The physicochemical properties of the voltage-gated sodium channel Nav1.6 protein revealed the number of amino acid be 1978 and the theoretical isoelectric point as 5.96. The maximum number of amino acids present in the sequence was found to be that of leucine (9.7%) and the least was that of histidine (1.3%). The instability index of the protein was 39.71. The number of negatively and positively charged residues is 234 and 216, respectively. The specific physical and chemical properties of both VGSc Nav1.6 and VGSc Na1.2 are displayed on Table 1.

To prevent residue side-chain orientation problems after homology modeling and repairing distorted geometries by moving atoms to release internal constraints, we used minimization algorithms in order to obtain the lowest energy of residue side-chain positions (Cagdas et al., 2011). RSMD value of the residue side-chains was 0.6 Å after minimization steps. To validate our approach and check refined models, we used Swiss-model structure assessment tool to validate the predicted model. Swiss-model QMEAN6 (Benkert et al., 2011) is a composite scoring function for both the estimation of the global quality of the entire model predicted with esypred3D server, as well as for the local per-residue analysis of different regions within a model; the results showed a value of 0.725, which is a high score ranging from 0 to 1.

3.2. Homology modeling of human voltage-gated sodium channel Nav1.6

We obtained the 3D model of the Nav1.6 channel (Fig. 2) by using the homology modeling server Esypred3D (Lambert et al., 2002), based on the crystal structure of C-terminal EF-hand

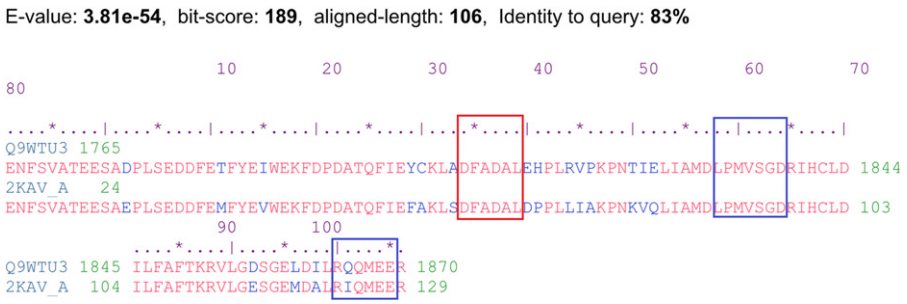

Fig. 1. The alignment results by using CLUSTALW6 (Thompson et al., 1994) showed a domain with unknown function (DUF3451). This presumed domain is functionally uncharacterized, and is commonly found in eukaryotes (blue square) and is compounded by ARG 1876, ILE 1877, GLN 1878, MET 1879, GLU 1880 and GLU 1881. The red squared sequence is a sodium ion transport-associated domain compounded by ASP 1806, PRO 1807, ASP 1808, ALA 1809, THR 1810 and GLN 1811. Members of this family contain a region found exclusively in eukaryotic sodium channels or their subunits, many of which are voltage-gated. This evidence suggests similar functions of both channels and gives the first step to validate it as a homology model of the human voltage-gated sodium channel Nav1.6. (For interpretation of the references to color in this figure legend, the reader is referred to the web version of this article.)

Table 1
Physical and chemical properties of the voltage-gated sodium channel Nav1.6 alpha subunit and its homologous, the voltage-gated sodium channel Nav1.2, obtained by analyzing their amino acid sequences using ProtParam server (Gasteiger et al., 2005). This information is relevant for validating the superposed structures, to integrate information of both molecules, and help understanding the similarity of both channels. The homologous channel in the right displays data not so far from the predicted model on the left part of the table. Pi, the total number of atoms and the GRAVY constant pointed both to be homologous.

Physical and chemical properties	**Molecules**	
	VGSc Nav1.6	**VGSc Nav1.2**
Theoretical pI	5.50	5.56
Molecular weight	258,995.0	227,974.8
Formula	$C_{10241}H_{15942}N_{2646}O_{2953}S_{11}$	$C_{645}H_{983}N_{171}O_{199}S_8$
Total number of atoms	31,893	32,133
Grand average of hydropathicity (GRAVY)	−0.001	−0.002

domain of human cardiac sodium channel Nav1.6 (PDB Entry: 2KBI_A) as template. The voltage-gated sodium channel Nav1.2 crystal structure properties are displayed on Table 1.

3.3. Chemical properties of Riluzole

Chemical characteristics of Riluzole were originally retrieved from Drug Bank database (Knox et al., 2010) and are displayed on Table 2, and its chemical structure is displayed on Fig. 1. This information taken from this public data bank, which is a chemoinformatics resource, is required for building the molecule of Riluzole and obtaining the 3D structure for the docking analysis. We obtained the detailed chemical, pharmacological and pharmaceutical drug information, and we also identified the main target being the voltage-gated sodium channel the most important.

The physicochemical properties of the Riluzole revealed the number of atoms to be 20. The molecule type points Riluzole as small molecule or small ligand; the molecular weight is 234.19831 (g/mol); Its chemical formula and (IUPAC) Name is C8H5F3N2OS and 6-(trifluoromethoxy)-1,3-benzothiazol-2-amine, respectively, riluzole is classified as phenols and derivatives, specifically described as benzothiazole family Fig. 3.

3.4. Binding sites of the voltage-gated sodium channel

According to the Q-site finder server (Laurie and Jackson, 2005) the predicted volume of the binding sites of the Nav1.6 homology model is 80 Å; protein volume is 9820 Å and its binding site residues are: 168 CD1 PHE 1786, 170 CE1 PHE 1786,172 CZ PHE 1786, **181 CE1 TYR 1787**, 182 CE2 TYR 1787, 183 CZ TYR 1787, 184 OH TYR 1787, **284 CB GLN 1799**, 285 CG GLN 1799. The predicted binding site are located on the transmembrane alpha

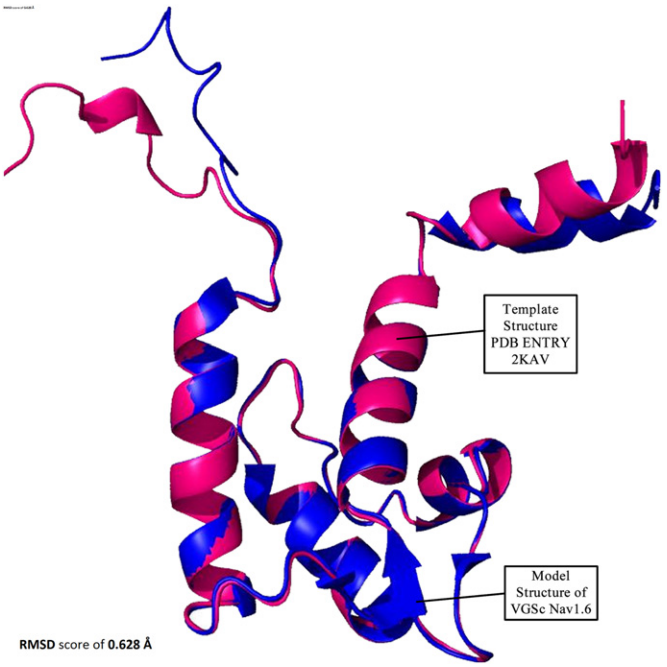

Fig. 2. Predicted theoretical model of the VGSC Nav1.6. The figure shows three domains of ion transport and one last domain of sodium ion transport. Results were obtained by using Esypred3D (Lambert et al., 2002). Advanced parameters were specified, establishing Nav1.6 (PDBentry: 2KAV) as a template for the prediction. The superimposed crystal structure of the voltage-gated sodium channel Nav1.2 (template), and the predicted 3D model of the Nav1.6 channel were modeled and superposed with PyMOL, with cartoon illustration and white background assigned. The superposition was also obtained and results revealed a score of 0.628 Å.

Table 2
The voltage-gated sodium channel alpha subunit Nav1.6 [*Homo sapiens*] alignment with the crystal structure of the voltage-gated sodium channel Nav1.2. Detailed information of the most flexible residues of the Nav1.6 predicted structure obtained by using the El Nemo program (Suhre and Sanejouad, 2004) is shown. Marked amino acids (red square) are the most flexible residues in the channel and may reveal a possible binding site. TYR 1787, LEU 1843 and GLN 1799 are the residues implicated in the docking complex, and this information was used for the docking protocol by using Autodock4.2 program (MacroModel, 2011), which requires the information of the flexible residues that had been now recognized.

Amino acid	Number	R^2
TYR	1787	0.0189
LEU	1843	0.0060
GLN	1799	0.0132
GLU	1765	0.1425
ASN	1766	0.1257
PHE	1767	0.1384
SER	1768	0.1053
VAL	1769	0.1781

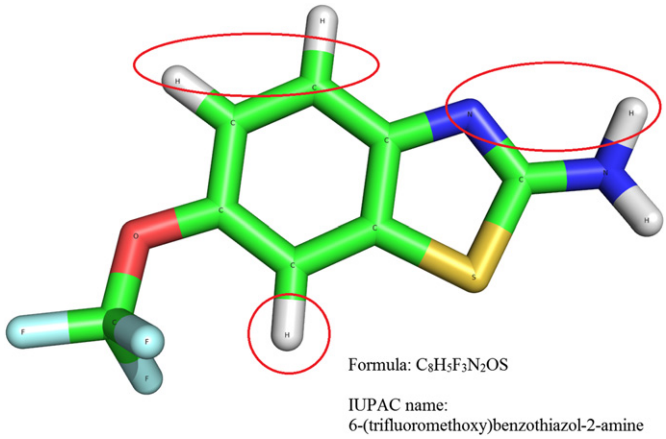

Fig. 3. Chemical structure of Riluzole (Drug Bank). Riluzole is composed by three atoms of phosphorus, three non-polar hydrogens, seven aromatic carbons, one amine functional group, one atom of sulfur, and one last of nitrogen. Its chemical formula is $C_8H_5F_3N_2OS$. The 2D structure was assessed by Acdlabs software (ACD/ChemSketch, 2012) by using the information obtained from the Drug Bank database, (Knox et al., 2010) and then converted into 3D format by Open Babel software (O'Boyle et al., 2011). The 3D structure was assessed by PyMOL program (Schrödinger, 2011), and element symbols were labeled for contact understanding. The contacts displayed (red circle) are the key contacts of the Riluzol with the predicted homology modeled voltage-gated sodium channel. (For interpretation of the references to color in this figure legend, the reader is referred to the web version of this article.)

helix S4 and S5 (Fig. 4), according to the previous report (Duclohier, 2009) with the voltage-gated sodium channel crystal structure prediction.

3.5. Determination of folding pattern

PFP-Pred (Shen and Chou, 2006), the protein fold prediction server describes the folding type of a protein. The results indicated that the folding type of the homology model predicted Nav1.6 was cupredoxins (Chou, 2004).

3.6. Computation of flexibilities of VGSc and Riluzole

Normal mode analysis (NMA) is a powerful tool for predicting the possible flexibilities of a given macromolecule. We used El Nemo (elastic network model) (Suhre and Sanejouad, 2004), a web interface to measure flexibilities of the Riluzole upon binding to the channel during docking simulations (Table 2).

3.7. Molecular docking simulations of Riluzole with the VGSc Nav1.6

The molecular docking interactions were obtained with Autodock v4.2 program (MacroModel, 2011) and performed with PyMOL, which is a Python-enhanced molecular graphics tool. We assessed the 3D visualization of the protein with a transparent surface, and developed the view of the Riluzole as 3D sticks labeling the element symbol to determinate the binding atoms related. Later we edited the view by displaying dotted polar contacts in both molecules (Figs. 5 and 6). The main interacting residues were Tyrosine 1787 (H=2.5 Å N=2.9 Å), LEU 1843 (O–N=2.9 Å) and GLN 1799 (O–O=3.1 Å).

3.8. Explicit solvent simulations

Structural aspects of the simulations of voltage-gated sodium channel are formed as symmetric dimers in solution, with three strands from each monomer (Ackerman and Clapham, 1997). The secondary structure of the channel (Schrödinger, 2011) is shown in Fig. 2. A primary distinction between the implicit solvent structure and that from homology modeling of VGSc Nav 1.6 lies on the distance between the helices (Jorgensen, 1982), as shown in Fig. 7. The center distance is about 37.9 Å in the homology modeled approach structure and about 39.3 Å in the implicit solvent results. The explicit water simulations began from the implicit solvent structure obtained by UCSF Chimera (Pettersen et al., 2004), but each moved within about 200 ps toward a structure with a helix–helix distance closer to that seen in the homology modeling structure (Fig. 8). This procedure also added 9.697 water molecules in the predicted model of the voltage-gated sodium channel Nav1.6 (Srinivasan et al., 1999).

The fluctuations in the distance are somehow important to determine the variation of the non-implicit solvent structure compared with the implicit one (Fig. 7) (Srinivasan et al., 1999), demonstrating the volume and direct–indirect contacts variation when including solvent in the simulation.

A secondary distinction is determined by the RMSD values variation in an implicit and non-implicit solvent docking environment (Srinivasan et al., 1999). The initial value (non-implicit solvent) ranged from 0.628 Å to 0.542 Å.

3.9. Refinement and complex validation

Comparison of template and the built model showed low differences with a root mean square deviation (RMSD) of 0.628 Å. Ramachandran plot from PROCHECK (Laskowski et al., 1993) was employed to examine the stereochemical quality of the built model. Result indicates that more than 85.3% of the residues have phi and psi angles in the most favored regions. An overall *G*-factor of −0.15 indicates a good quality of the built model. The residues in the disallowed region were located outside of the binding pocket, thus no further action was taken to further improve the backbone folding of these residues. The validation of the built model was again confirmed by secondary structure calculation on the built model.

The energy minimization result of the docked complexes went from an initial total energy of 65,998 kJ/mol to −34,776 kJ/mol. For high-quality test set validation of protein-ligand and docking performance, we used the server POLYVIEW MM. Our results confirmed the obtained docked complex and indicated that contacting residues were Y1787 Q1799 H1841 C1842 L1843 Y1787 Q1799 H1841 C1842 L1843. Furthermore, these docking results by Autodock4.2 server reported three specific amino acids that may be interacting in the docked complex (THY 1787, LEU 1843 and GLN 1799).

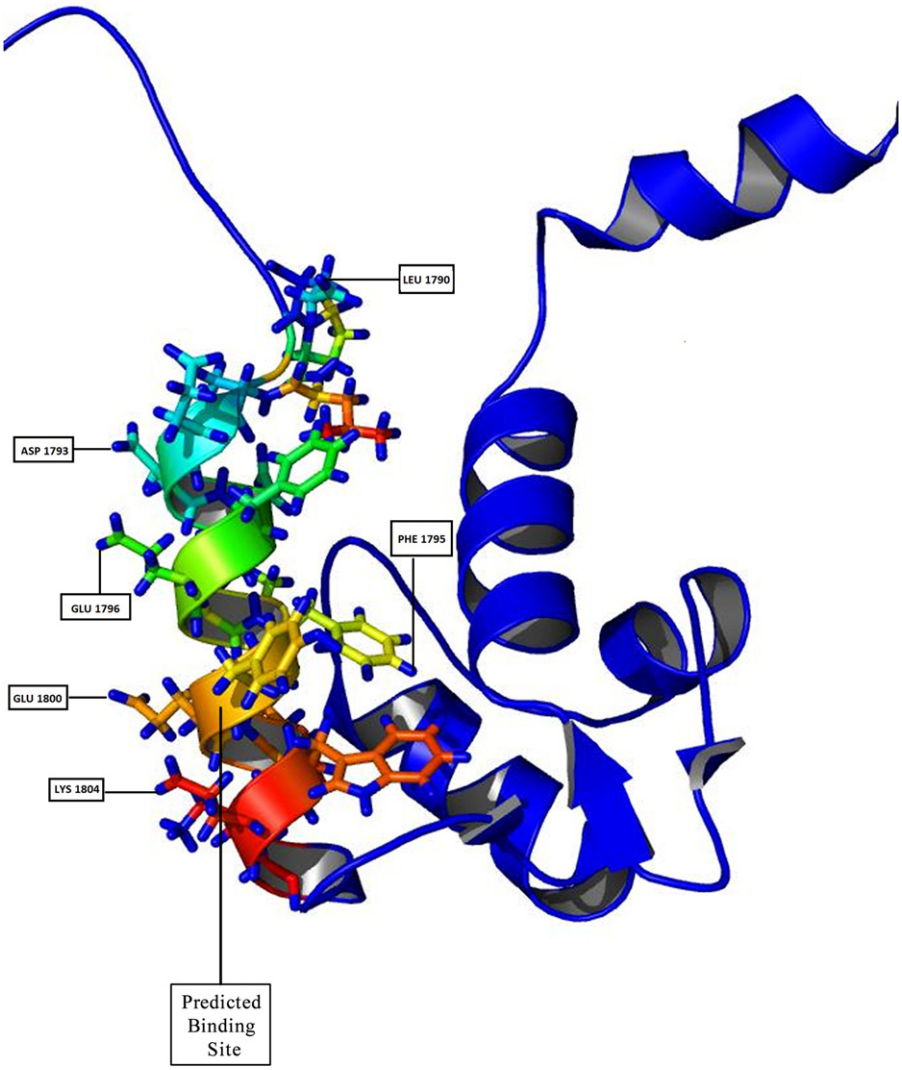

Fig. 4. Predicted binding sites obtained by using the software Q-site finder (Laurie and Jackson, 2005). The possible binding sites of selected target receptors were searched to predict the ligands binding sites. It works by binding hydrophobic probes to the protein and finding clusters of probes with the most favorable binding energy (Bairoch and Apweiler, 1997). The blue colored zone of the voltage-gated sodium channel is assembled with the key interacting amino acids and created a surface where Riluzole is probably binding. (For interpretation of the references to color in this figure legend, the reader is referred to the web version of this article.)

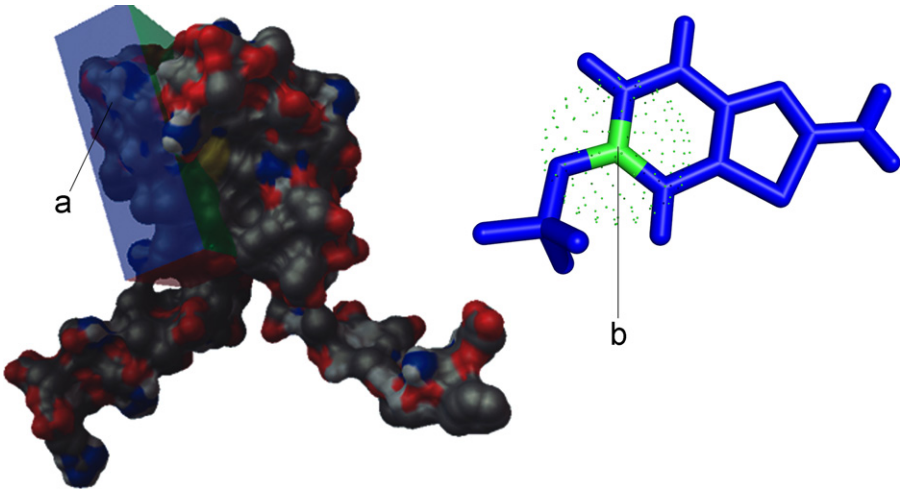

Fig. 5. (a) Searching grid extended over the selected target protein, Nav1.6 channel. The grid was performed following some parameters: *X* dimension number of points: 38; *Y* dimension number of points 40; *Z* dimension number of points and spacing of 0.375 Å, The grid was extended following the parameters of the El Nemo results and the transmembrane region was detected, based on previous findings (Duclohier, 2009). (b) The selected root of the ligand (Riluzole), which is located on the 6th aromatic carbon of this compound, was detected by using Autodock v4.2 program. This program automatically detects the most probable atom to be the most likely torsioned.

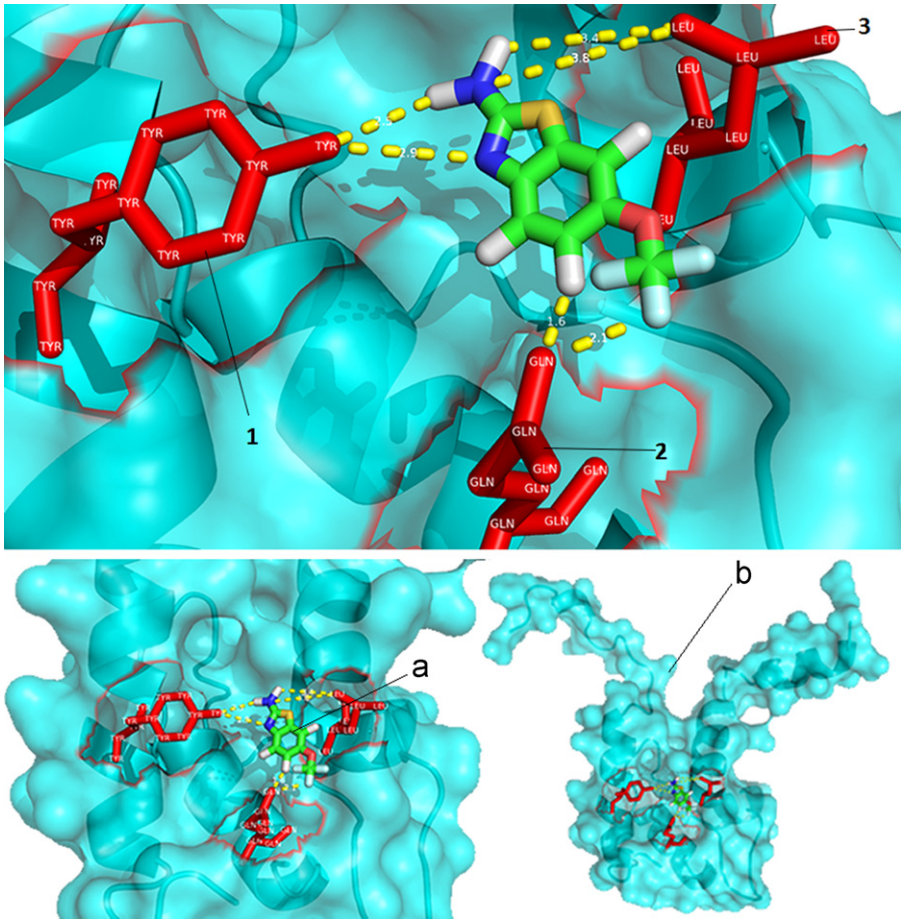

Fig. 6. (a) Riluzole binding to the VGSc Nav1.6, (b) the surface of the VGSc Nav1.6 interacting with Riluzole. (1) Nitrogen and hydrogen atoms from the Riluzole structure interacting with the voltage-gated sodium channel by the tyrosine 1787 terminal oxygen. Polar interactions are shown as dotted lines. (2) Glycine 1799 was interacting with Riluzole by polar contacts (glycine oxygen with both hydrogens of Riluzole). (3) Hydrogen from the Riluzole was interacting by polar contact (yellow dotted lines) with leucine 1943 on VGSc Nav1.6. Three polar interactions between VGSc Nav1.6 and Riluzole included TYR 1787 (H=2.5 Å N=2.9 Å), LEU 1843 (O–N=2.9 Å) and GLN 1799 (O–O=3.1 Å). (For interpretation of the references to color in this figure legend, the reader is referred to the web version of this article.)

3.10. Transmembrane residues

The sequence alignment result of the transmembrane region of Nav1.2 and the Nav1.6 showed 100% of coverage, which revealed the transmembrane region, located between the **ASP 1831** and the **LEU 1854** where Riluzole may be binding (Fig. 9).

4. Discussion

The main purpose of this study was to determine the complex structure of Riluzole with the VGSc Nav1.6. Based on the homology model voltage-gated sodium channel, brain isoform (Nav1.2), we have investigated the recognition pattern between Riluzole and the sodium channel Nav1.6 by combining homology modeling and docking simulations. The homology modeling results presented a RMSD (root-mean-square deviation) of 0.628 Å, which is a good measurement of the average distance between atoms (backbone atoms; (Damm et al., 2006)) of the superimposed protein Nav1.2 and the predicted model of the voltage-gated sodium channel. This result ensures that the homology model was predicted with high accuracy and may be used as a template for further investigations (Maiti et al., 2004).

The folding pattern is a significant way to determinate the accuracy of a predicted structure (Savelieff et al., 2008). The correct 3D structure is essential for functions determination (Syed et al., 2012), although some parts of functional proteins may remain unfolded and failure to folding into native structure produces inactive or inaccurate proteins (Mehta et al., 2012). In this context, the folding pattern becomes an important tool to integrate the previous analysis and to prove the predicted model of the voltage-gated sodium channel functions by driving its natural role in cellular functions and metabolism. In this study, the folding pattern was found to be cupredotoxins, which is an important motif in numerous proteins that are central to several critical cellular processes (Savelieff et al., 2008), including fluctuation in iron-mediated processes and sodium ions exchanging (Mehta et al., 2012). This demonstrates that the predicted model shares the same functions with its natural state model. On the other hand, sodium, a highly reactive metal and a member of the alkali metals, is the main (Gatti et al., 2010) implicated ion in voltage-gated channel, as the latter controls sodium ions (Na^+) gradient through plasma membrane (Catterall et al., 2005). This approves that the predicted voltage-gated sodium channel folding pattern meets the functions related and this prediction is validated for further analysis.

The three interacting residues of the voltage-gated sodium channel Nav1.6, TYR 1787, LEU 1843 and GLN 1799, are the key residues with the most favorable binding energy, suggesting that these residues may be part of the protein active site. Tyrosine is considered as a polar amino acid that interacts with the Riluzole in its polar region, as shown on Fig. 6. Meanwhile leucine and glycine are non-polar amino acids that also bind to this molecule. According to these results, Riluzole appears to dock on the voltage

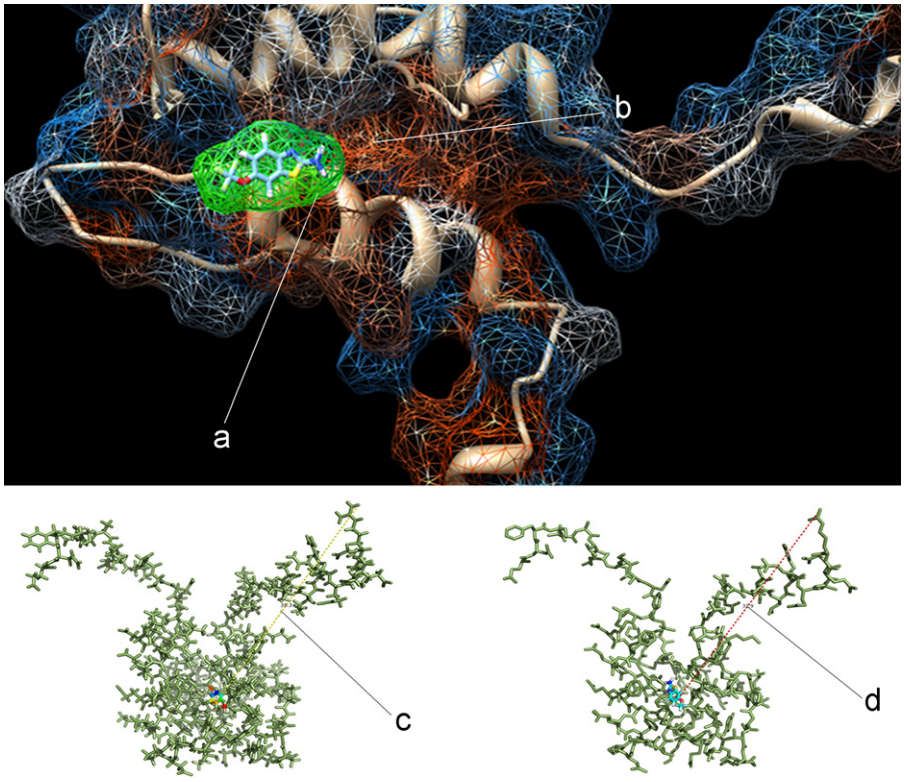

Fig. 7. (a) and (b) are the results from the MDFF and UCSF Chimera (Pettersen et al., 2004) program of implicit solvent analysis. (a) Riluzole molecule binding on an implicit solvent environment was assessed by the chimeras long-range electrostatic interactions, (b) voltage-gated sodium channel under energy fluctuations and kinetic energy by the implicit solvent analysis. ((c) yellow line) and ((d) red line) represent a primary distinction between the implicit solvent structure and that from homology modeled structure of VGSc Nav1.6, lying on the distance between the helices. The center to opposite end distance is about 39.3 Å and 37.9 Å, respectively. (For interpretation of the references to color in this figure legend, the reader is referred to the web version of this article.)

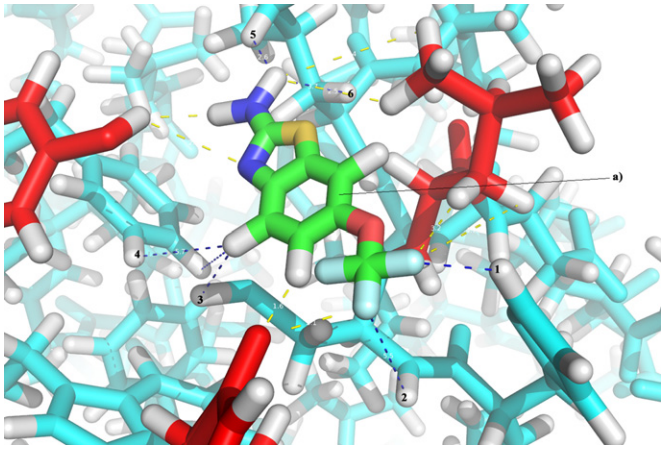

Fig. 8. (a) Embedded structure of Riluzole into a water box of the voltage gated sodium channel Nav1.6 using the solvate plugin in a neutrally charged system. This was done by neutralizing counterions to the simulation system following the UCSF Chimera Pettersen et al., 2004 software parameters. Numbers from 1 to 6 are the non-direct contacts pointed by Chimera software with implicit solvent docked solutions. Numbers 5 and 6 are non-direct contacts colored by blues, and are the nearest contacts with 2.6 Å and 2.5 Å, respectively. (For interpretation of the references to color in this figure legend, the reader is referred to the web version of this article.)

gated channel by polar contacts. However, it does not seem to deeply enter the ion channel pore, which may be due to the fact that Riluzole is positively charged (Polarity: 18.59) (Wang et al., 2008). As in such way, Riluzole enters the channel, this would lead to some electrostatic repulsion and a resultant loss of affinity (Risterucci et al., 2006). Previous report supports this hypothesis by suggesting that Riluzole may be binding to the transmembrane alpha helix, instead of the pore region (Miller et al., 2012).

One of the key residues in the interaction of Nav1.6 with Riluzole is tyrosine, a non-essential amino acid implicated in important biological processes (ACD/ChemSketch, 2012). We found Riluzole to be interacting with this amino acid located in the Nav1.6 binding site, thus suggesting an important functional regulation at cellular level with an r^2 of 0.0189, demonstrating a high affinity of Riluzole with this amino acid in the active site (Table 2). Another binding interacting amino acid is leucine, a branched-chain α-amino acid (Melnik, 2012), that docks to the VGSc Nav1.6 by its atom of terminal carbon (Nikolaev and Pervushin, 2012). Furthermore, leucine, the second interacting key residue with Riluzole, has been considered as an important residue interacting with this type of channel. Our results showed that Riluzole may be binding to leucine residues with an $r^2=0.0060$, suggesting a possible and specific interaction with this drug.

Previous studies confirmed the hypothesis that the residues phenylalanine 1710 and tyrosine 1787 (TYR 1787, as also shown in the present study, from VGSC Nav1.6 were identified as residues implicated in Riluzole binding activity (Denac et al., 2000). These residues were proposed to face toward the channel pore during binding of drugs, as Riluzole (Song et al., 1997). This implies that the local receptor site is located in the pore of the channel. According to this model the local binding site should be physically close to the selectivity filter of the VGSCs and to the binding site of the inactivation gate (Denac et al., 2000). In addition, after identification of this intracellular region as inactivation gate, a cluster of hydrophobic amino acids was found to play a crucial role (Duclohier, 2009). This cluster, containing leucine 1843, phenylalanine 1489 and methionine 1490, has been identified as a fragment required for sodium channel inactivation (Mantegazza et al., 2010). These

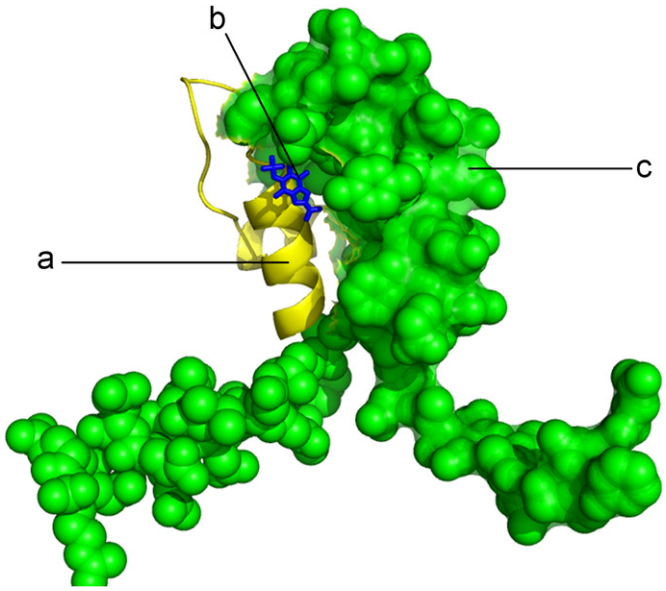

Fig. 9. (a) The pore region formed by the S5 segment, which is the transmembrane region of the homology modeled Nav1.6, (b) Riluzole binding to the linker residues of the channel in the transmembrane region composed by the linker (transmembrane) residues on the VGSC (Nav1.6), (c) the non-linker site transmembrane region of the voltage-gated sodium channel Nav1.6, both detected by an alignment with Clustalw (Larkin, 2007). (For interpretation of the references to color in this figure legend, the reader is referred to the web version of this article.)

findings support the hypothesis that part of the receptor of the VGSCs is formed by the amino acid residues, leucine and tyrosine (position 1843 and 1787), in domain DIV transmembrane segment S6 of the α-subunit of Nav1.6 (Ragdale et al., 1996).

We report here that the main interacting residues of VGSc Nav1.6 with Riluzole were Leucine, Tyrosine and Glycine. However, Glycine has not been experimentally reported as a main interacting residue with Riluzole. We found binding energy of glycine 1799 with Riluzole to be 3.1 Å (Jorgensen and Tirado-Rives, 1988), which may somehow demonstrate a strong interaction with high affinity (Saeed et al., 2012). Glycine is believed to be a key pharmacophore in several ion channels studies. Normally, glycine acts as a ligand trigger to open ion channels in the CNS, and any mutation on glycine residues may interfere with channel control of ions gradients, leading to uncontrolled influx into to the cell, which somehow mimics specific symptoms in ALS (Alvaro et al., 1995). However, for the voltage-gated sodium channel Nav1.6, this process has not been previously reported, but it seems clear that this process may likely occur, as it shares numerous conserved domains and related functions with other ion channels (Ackerman and Clapham, 1997).

To validate this approach in a more reliable way, implicit solvent docking simulations were assessed by using the UCSF Chimera software (Gerber et al., 2000). This method is often applied to estimate solute-solvent interactions in structural and chemical processes (Srinivasan et al., 1999). The implicit solvation model for the interaction of the voltage-gated sodium channel Nav1.6 with the 3D structure of the Riluzole was justified in water molecules, where the potential of mean force can be applied to approximate the average of dynamic solvent molecules (Schrödinger, 2011). Our approach showed three new results: (i) a center-side chain distance difference between the non-implicit and implicit solvent structures was 37.9 Å and 39.3 Å, respectively. This is an important measure to evaluate the coverage range of the new docking procedure (Schrödinger, 2011); (ii) the RMSD value ranged from 0.628 Å to 0.542 Å. This is a measure of how well the computer derived and experiment derived models overlap (Pettersen et al., 2004). As the RMSD value decreased, this may indicate a better predicted model of the voltage-gated sodium channel when solvents are implicit; and (iii) the interactions increased 60% when taking into account the implicit solvent. These results may somehow represent a more regular system, especially when assessing the non-direct and direct contacts by adding 9.697 water molecules, thus becoming a more reliable docking simulation (Srinivasan et al., 1999).

The beneficial use of Riluzole in ALS is commonly accredited to its anti-glutamatergic properties (Desiato et al., 1999). The side effects of Riluzole, such as drowsiness and adynamia, and anticonvulsant characteristics, suggest that inhibitory receptors are also involved in the action of Riluzole. The most widespread inhibitory receptors prevailing in the brain stem and spinal cord of mammals are both GABA receptor and glycine receptor (Jorgensen and Tirado-Rives, 1988). Interestingly, we show a potential interaction of Riluzole with the voltage-gated sodium channel on the polar glycine residues (Karp, 2001; Bahram et al., 2001). Glycine regulates important cellular functions, as this amino acid can be embedded in hydrophilic or hydrophobic environments, due to its two hydrogen atom side chains (Karp, 2001; Bahram et al., 2001). This finding is potentially important to be used as an output for the generation of newly designed medicines with some predetermined pharmacologic profiles in ALS (Araki et al., 2001). The results presented here seem to be relevant as we show (i) for the first time an interaction of Riluzole with the voltage-gated sodium channel Nav1.6 alpha sub-unit (Aggarwal and Cudkowicz, 2008), and (ii) predict a molecular model of interaction between Riluzole and glycine residues of the VGSc, as the latter is a neurophysiological target directly implicated in the progression of the disease (Karp, 2001; Bahram et al., 2001). Since Riluzole may act on sodium channels, the results presented here serve as an important output for better drug design targeting a more and effective therapeutically response to ALS progression in patients.

Acknowledgements

This work was supported in part by PUJ grants IDs 4327 and 4367 to GEB and ID 4783 to JG.

References

ACD/ChemSketch, Advanced Chemistry Development, Toronto, ON, Canada, 2012.
Ackerman, M., Clapham, D., 1997. Ion channels—basic science and clinical disease. Massachusetts Medical Society 336, 157–224.
Aggarwal, S., Cudkowicz, M., 2008. ALS drug development: reflections from the past and a way forward. Neurotherapeutics 5, 516–527.
Ahn, H., Choi, J., Choi, B., Kim, M., Rhie, D., SH, Y., Jo, Y., Kim, M., Sung, K., Hahn, S., 2005. Inhibition of the cloned delayed rectifier K^+ channels, Kv1.5 and Kv3.1, by riluzole. Neuroscience 133, 1007–1019.
Ajroud-Driss, S., Saeed, M., Khan, H., Siddique, N., Hung, W.Y., Sufit, R., Heller, S., Armstrong, J., Casey, P., Siddique, T., Lukas, T.J., 2007. Riluzole metabolism and CYP1A1/2 polymorphisms in patients with ALS. Amyotroph Lateral Scler. 8, 305–309.
Altschul, S., Madden, T., Schäffer, A., Zhang, J., Zhang, Z., Miller, W., Lipman, D., 1997. Gapped BLAST and PSI-BLAST: a new generation of protein database search programs. Nucleic Acids Res. 25, 3389–3402.
Alvaro, G., Estevez, A., Jean-Marie, S., Luis, B., 1995. Protective effect of riluzole on excitatory amino acid-mediated neurotoxicity in motoneuron-enriched cultures. Eur. J. Pharmacol. 280, 47–53.
Andrews, J., 2009. Amyotrophic lateral sclerosis: clinical management and research update. Curr. Neurol. Neurosci. Rep. 9, 59–68.
Araki, T., Kumagai, T., Tanaka, K., Matsubara, M., Kato, H., Itoyama, Y., Imai, Y., 2001. Neuroprotective effect of riluzole in MPTP-treated mice. Brain Res. 918, 176–181.
Azbill, M.XPlease provide the full name of autors.., Springer, R.D., 2000. J.E. Riluzole increases high-affinity glutamate uptake in rat spinal cord synaptosomes. Mol. Brain Res. 871 (2), 175–180.
Bahram, M., Klaus, K., Hafis, M., Reinhard, D., Johannes, B., 2001. Interaction of The Neuroprotective Drug Riluzole with GABAA and Glycine Receptor Channels. Eur. J. Pharmacol. 415, 135–140.

Bairoch, A., Apweiler, R., 1997. The Swiss-Prot protein sequence database: its relevance to human molecular medical research. Mol. Med. 75, 312–316.
Balamurugan, R., Stalin, A., Ignacimuthu, S., 2011. Molecular docking of g-sitosterol with some targets related to diabetes. Eur. J. Med. Chem. 47, 38–43.
Benkert, P., Biasini, M., Schwede, T., 2011. Toward the estimation of the absolute quality of individual protein structure models. Bioinformatics 27, 343–350.
Berman, H., Westbrook, J., Gilliland, F.Z.G., Bhat, T., Weissig, H., Shindyalov, I., Bourne, P., 2000. The Protein Data Bank. Nucleic Acids Res. 28, 235–242.
Cagdas, T., Miook, C., Yousin, S., 2011. Discovery of functional gene variants associated with human longevity: opportunities and challenge. J. Gerontol. 67A, 376–383.
Catterall, W., Goldin, A., Waxman, S., 2005. Nomenclature and structure–function relationships of voltage-gated sodium channels. Pharmacologica 57, 397–409.
Cheah, B., Vucic, S., Krishnan, A., Kiernan, M., 2010. Riluzole, neuroprotection and amyotrophic lateral sclerosis. Curr. Med. Chem. 17, 1942–1959.
Chou, K., 2004. Using amphiphilic pseudo amino acid composition to predict enzyme subfamily classes. Bioinformatics 21, 10–19.
Clark J., Pritchard C., Sunak S., 2005. Amyotrophic lateral sclerosis, a report on the state of research into the cause, cure, and prevention of ALS, the ALS Therapy Development Foundation, State of Massachusetts.
ClustalW, Larkin, ClustalX, 2007. Bioinformatics 23, 2947–2948.
Cornell, W., Cieplak, P., Bayly, C., Gould, I., Merz, K., Ferguson, D., Spellmeyer, D., Fox, T., Caldwell, J., Kollman, P., 1995. A second generation force field for the simulation of proteins, nucleic acids, and organic molecules. J. Am. Chem. Soc. 117, 5179–5197.
Cornell, W., Abseher, R., Nilges, M., Case, D.A., 2001. Continuum solvent molecular dynamics study of flexibility in interleukin-8. Novartis Pharmaceutical Corporation, USA 19, 136–145.
Damm, K.L., Carlson, H.A., 2006. Gaussian-weighted RMSD superposition of proteins: a structural comparison for flexible proteins and predicted protein structures. Biophys. J. 90, 4558–4573.
Denac, H., Mevissen, M., Scholtysik, G., 2000. Structure, function and pharmacology of voltage-gated sodium channels. Naunyn–Schmiedeberg's Arch. Pharmacol. 362, 453–479.
Desiato, M., Palmieri, T., Giacobini, M., Scalise, P., Arcipede, A., Caramia, F., 1999. The effect of riluzole in amyotrophic lateral sclerosis: a study with cortical stimulation. J. Neurol. Sci. 16, 98–107.
Diss, J., Archer, S., Hirano, J., Fraser, S., Djamgoz, M., 2001. Expression profiles of voltage-gated Na(+) channel alpha-subunit genes in rat and human prostate cancer cell lines. Prostate 48, 165–178.
Donovan, B., Bakshia, T., Galbraithb, S., Nixona, C., Paynec, L., Martensa, S., 2011. Utility of frozen cell lines in medium throughput electrophysiology screening of hERG and Nav1.5 blockade. J. Pharmacol. Toxicol. Methods 64, 269–276.
Duclohier, H., 2009. Structure–function studies on the voltage-gated sodium channel. Biochim. Biophys. Acta 1788, 2374–2379.
Dunlop, B.M.H., She, J., Howland, Y., 2003. Impaired spinal cord glutamate transport capacity and reduced sensitivity to riluzole in a transgenic superoxide dismutase mutant rat model of amyotrophic lateral sclerosis. J. Neurosci. 23, 1688–1696.
Foran, E., Trotti, D., 2009. Glutamate transporters and the excitotoxic path to motor neuron degeneration in amyotrophic lateral sclerosis. Antioxid Redox Signal 11, 1587–1602.
Fu, W., Cui, M., Briggs, J., Huang, X., Xiong, B., Zhang, Y., Luo, X., Shen, J., Ji, R., Jiang, H., Chen, K., 2002. Brownian dynamics simulations of the recognition of the scorpion toxin maurotoxin with the voltage-gated potassium ion channels. Biophys. J. 83, 2370–2385.
Gasteiger, E., Hoogland, C., Gattiker, A., Duvaud, S., Wilkins, M.R., Appel, R.D., Bairoch, A., 2005. In: Press, H. (Ed.), Protein Identification and Analysis Tools on the ExPASy Server. The Proteomics Protocols Handbook, pp. 571–607.
Gatti, M., Tokatly, I., Rubio, A., 2010. Sodium: a charge-transfer insulator at high pressures. Phys. Rev. Lett. 104, 216–404.
Gerber, N., Lowman, H., Artis, D.R., Eigenbrot, C., 2000. Receptor-binding conformation of the ELR motif of IL-8: X-ray structure of the L5C/H33C variant at 2.35 resolution. Proteins 38, 361–367.
Hartshorn, M., Verdonk, M., Chessari, G., Brewerton, S., Mooij, W., Mortenson, P., Murray, C., 2007. Diverse, high-quality test set for the validation of protein-ligand docking performance. J. Med. Chem. 50, 726–741.
Hebert, T., Drapeau, P., Pradier, L., Dunn, R., 1994. Block of the rat brain IIA sodium channel alpha subunit by the neuroprotective drug riluzole. Mol. Pharmacol., 1055–1060.
Hoffman, J.J., 2008. Toward a better understanding of amyotrophic lateral sclerosis. Home Healthcare Nurse 26, 337–342.
Jorgensen, W., 1982. Solvation and conformation of methanol in water. Chem. Phys. 77, 4156.
Jorgensen, W., Tirado-Rives, J., 1988. The OPLS [optimized potentials for liquid simulations] potential functions for proteins, energy minimizations for crystals of cyclic peptides and crambin. J. Am. Chem. Soc. 110, 1657–1666.
Karp, G., 2009. Cell and molecular biology: concepts and experiments. John Wiley & Sons Inc.
Knox, C., Law, V., Jewison, T., Liu, P., Ly, S., Frolkis, A., Pon, A., Banco, K., Mak, C., Neveu, V., Djoumbou, Y., Eisner, R., AC, G., Wishart, D., 2010. DrugBank 3.0: a comprehensive resource for 'Omics' research on drugs. Nucleic Acids Res. 39, D1035–D1041.
Lambert, L.N., De Bolle, C., Depiereux, X., ESyPred3D, E., 2002. Prediction of proteins 3D structures. Bioinformatics 18, 1250–1256.
Laskowski, R.A., MacArthur, M.W., Moss, D.S., Thornton, J.M., 1993. PROCHECK: a program to check the stereochemical quality of protein structures. J. Appl. Crystallogr. 26, 283–291.
Laurie, A., Jackson, R., 2005. Q-site finder: an energy-based method for the prediction of protein–ligand binding sites. Bioinformatics 21, 1908–1916.
Liu, S., Zhang, C., Zhou, H., Zhou, Y., 2004. A physical reference state unifies the structure-derived potential of mean force for protein folding and binding. Proteins 56, 93–101.
MacroModel, Schrödinger, LLC, New York, 2011.
Maiti, R.G.H.V.D., Zhang, Haiyan, David, S., 2004. Wishart*, SuperPose: a simple server for sophisticated structural superposition. Nucleic Acids Res. 32, W590–W594.
Mantegazza, M., Curia, G., Biagini, G., Ragsdale, D., Avoli, M., 2010. Voltage-gated sodium channels as therapeutic targets in epilepsy and other neurological disorders. Lancet Neurol. 9, 413–424.
McGuire, D., Garrison, L., Armon, C., Barohn, R.J., Bryan, W.W., Miller, R., Parry, G.J., Petajan, J.H., Ross, M.A., 1997. A brief quality-of-life measure for ALS clinical trials based on a subset of items from the sickness impact profile. The Syntex–Synergen ALS/CNTF Study Group. J. Neurol. Sci. 152, 18–22.
Mehta, R., Hawthorne, M., Peng, X., Shilkaitis, A., Mehta, R., Beattie, C., Das Gupta, T., 2012. A 28-amino-acid peptide fragment of the cupredoxin azurin prevents carcinogen-induced mouse mammary lesion. AACR J. 3, 1351–1360.
Melnik, B.C., 2012. Leucine signaling in the pathogenesis of type 2 diabetes and obesity. World J. Diabetes 3, 38–53.
Miller, R., Mitchell, D., Lyon, M., Moore, D., 2012. Riluzole for amyotrophic lateral sclerosis (ALS)/motor neuron disease (MND). Cochrane Database Syst. Rev. 3.
Morris, A., MacArthur, M., Hutchinson, E., Thornton, J., 1992. Stereochemical quality of protein structure coordinates. Proteins 12, 345–364.
Nikolaev, Y., Pervushin, K., 2012. Structural basis of RNA binding by leucine zipper GCN4. Protein Sci. 21, 667–676.
Norris, F.H., Denys, E.H., Sang, K., Mukai, E., 1989. The natural history of ALS in a specified population, with comments on risk factors, prognosis and symptomatic treatments. Rinsho Shinkeigaku 29, 1485–1492.
O'Boyle, M., Banck, M., James, C., Morley, C., Vandermeersch, T., Hutchison, G., 2011. Open Babel: an open chemical toolbox. J. Cheminf. 33, 1186–1758.
Pettersen, E., Goddard, D., Huang, C., Couch, S., Greenblatt, M., Meng, C., Ferrin., E., 2004. Comput. Chem. 13, 1605–1612.
Ragdale, D., Mcphee, J., Scheuer, T., William, A., Cattellar, D., 1996. Common molecular determinants of local anesthetic,antiarrhythmic, and anticonvulsant block of voltage-gated Na^+ channels. Pharmacology 93, 9270–9275.
Risterucci, C., Coccurelloa, R., Banasrb, M., Stutzmannc, J., Amalrica, M., Nieoullonb, A., 2006. MPEP and the Na^+ channel blocker riluzole show different neuroprotective profiles in reversing behavioral deficits induced by excitotoxic prefrontal cortex lesions. Neuroscience 137, 211–220.
Saeed, U., Nawaz, N., Waheed, Y., Chaudry, N., Tariq Bhatti, H., Urooj, S., Waheed, H., 2012. In silico identification of BIM-1 (2-methyl-1*H*-indol-3-yl) as a potential therapeutic agent against elevated protein kinase C beta associated diseases. Afr. J. Biotech. 11, 4434–4441.
Savelieff, M., Wilson, T., Elias, Y., Nilges, M., Garner, D., Lu, Y., 2008. Experimental evidence for a link among cupredoxins: red, blue, and purple copper transformations in nitrous oxide reductase. Proc. Nat. Acad. Sci. U.S.A. 105, 7919–7924.
Schrödinger, L., 2011. The PyMOL Molecular Graphics System.
Schwartz, G., Fehlings, M.G., 2002. Secondary injury mechanisms of spinal cord trauma: a noveltherapeutic approach for the management of secondary pathophysiology with the sodium channel blocker riluzole. Prog. Brain Res. 137, 177–190.
Shashank, D., 2003. Voltage-gated sodium channel modulation of calcium dynamics and NMDA receptor signaling in murine neocortical neuron, Faculty of Phylosophy, The University of Georgia. Athens Giogia, 170.
Shen, H., Chou, K., 2006. Ensemble classifier for protein fold pattern recognition. Bioinformatics 22, 1717–1722.
Song, J., Sheng Huang, C., Nagata, G., Yeh, J.Z., Narahashi, T., 1997. Differential action of riluzole on tetrodotoxin-sensitive and tetrodotoxin-resistant sodium channels. J. Pharmacol. Exp. Ther. 282, 707–714.
Srinivasan, J., Trevathan, M.W., Beroza, P., Case, D.A., 1999. Application of a pairwise generalized Born model to proteins and nucleic acids: Inclusion of salt effects. Theor. Chem. Acc. 101, 426–434.
Suhre, K., Sanejouad, Y., 2004. ElNémo: a normal mode web server for protein movement analysis and the generation of templates for molecular replacement. Nucleic Acids Res. 32, W610–W614.
Syed, R., Rani, R., Sabeena, A., Ahmad Masoodi, T., Shafi, G., Alharbi, K., 2012. Functional analysis and structure determination of alkaline protease from Aspergillus flavus. Bioinformation 8, 175–180.
Tarnawa, I., Bölcskei, H., Kocsi, P., 2007. Blockers of voltage-gated sodium channels for the treatment of central nervous system disease. Recent Pat. CNS Drug Discovery 2, 57–78.
Tavakoli, M., 2002. Disease progression in amyotrophic lateral sclerosis identifying the cost-utility of riluzole by disease stage. Eur. J. Health Econ. 3, 156–165.
Thompson, J., Higgins, D., Gibson, T., 1994. CLUSTAL W: improving the sensitivity of progressive multiple sequence alignment through sequence weighting, position-specific gap penalties and weight matrix choice. Nucleic Acids Res. 22, 4673–4680.
Tsui, V., Case, D.A., 2000. Molecular dynamics simulations of nucleic acids using a generalized Born solvation model. J. Am. Chem Soc. 122, 2489–2498.

Tytgat, J., Peigneur, S., 2012. The sophisticated peptide chemistry of venomous animals as a source of novel insecticides acting on voltage-gated sodium channels, Insecticides—advances in integrated pest management. Intech.

Van Den Bosch, L., Van Damme, P., Bogaert, E., Robberecht, W., 2006. The role of excitotoxicity in the pathogenesis of amyotrophic lateral sclerosis. Biochim. Biophys. Acta 1762, 1068–1082.

Wallace, A., Laskowski, R., Thornton, J., 1996. Derivation of 3D coordinate templates for searching structural databases: application to Ser-His-Asp catalytic triads in the serine proteinases and lipases. Protein Sci. 5, 1001–1101.

Wang, Y., Lin, M., Lin, A., Wu, S., 2008. Riluzole-induced block of voltage-gated Na^+ current and activation of BKCa channels in cultured differentiated human skeletal muscle cells. Life Sci. 82, 11–20.

Wokke, J., 1996. Riluzole. Lancet 348, 1660–1661.

Yiangou, Y., Facer, P., Chessell, I.P., Bountra, C., Chan, C., Fertleman, C., Smith, V., Anand, P., 2007. Voltage-gated ion channel Nav1.7 innervation in patients with idiopathic rectal hypersensitivity and paroxysmal extreme pain disorder (familial rectal pain). Neurosci. Lett. 427, 77–82.